Analytical Understanding of Multiple-Angle Incidence Resolution Spectrometry Based on a Classical Electromagnetic Theory

Yuki Itoh, Akiyoshi Kasuya, and Takeshi Hasegawa*

Department of Chemistry, Graduate School of Science and Engineering, Tokyo Institute of Technology, 2-12-1 Ookayama, Meguro-ku, Tokyo 152-8551, Japan

Received: April 23, 2009; Revised Manuscript Received: May 18, 2009

Infrared multiple-angle incidence resolution spectrometry (IR-MAIRS) is a unique spectroscopic technique to retrieve both surface-parallel (in-plane; IP) and -perpendicular (out-of-plane; OP) molecular vibration spectra simultaneously from an identical thin-film deposited on a high refractive index substrate, and the measurement theory was constructed by the use of a theoretical framework of regression equation. The core part of the MAIRS theory is found in the weighting factor matrix, **R**, used for a linear combination, which was constructed in an unusual manner. Because a regression equation does not strictly correlate the left- and right-hand sides of the equation, **R** matrix cannot directly be deduced from Maxwell's equation. Although the conventional studies using IR-MAIRS gave excellent empirical results, a strict physical understanding of MAIRS is necessary; otherwise, we cannot rely on it at least quantitatively. In the present study, the MAIRS theory has first been analyzed by the use of Maxwell's equations inductively. As a result, both MAIRS-IP and -OP spectra have readily been expressed as a linear combination of the $\mathrm{Im}(\boldsymbol{\varepsilon}_x)$ and $\mathrm{Im}(-1/\boldsymbol{\varepsilon}_z)$ functions that correspond to the conventional transmission and reflection−absorption spectra. Through the analysis of coefficients of the linear combination, MAIRS has proved to be reliably useful for analysis of thin film on a high refractive index substrate.

Introduction

Quantitative understanding of infrared spectra of thin films has long been an analytical topic, and many analytical approaches have been proposed on the basis of the classical electromagnetic theory starting from Maxwell's equations. The earliest successful analytical theory was proposed by Abelés, who developed the transfer-matrix[1,2] (or known as M-matrix[3]) method, which drastically simplifies a calculation process of transmission and reflection spectra of an accumulated thin film (stratified medium). Although this theoretical calculus is useful for any films made of heterogeneous stratified multilayers, the calculus has an analytical limit that only optically isotropic media can be analyzed. Therefore, molecular orientation analysis in a film cannot be performed with the technique in principle because molecular orientation yields optical anisotropy.

This analytical procedure can be simplified by Taylor expansion in terms of the film thickness over the wavelength, within the limit that only three-layer (such as air/film/substrate) medium can be treated.[4] The Taylor-expanded approximation equation was later divided into two components by Hansen, which correspond to the surface-parallel (in-plane; IP) and -perpendicular (out-of-plane; OP) optical parameters.[4] Because coding of Hansen's approximation equations on a computer was very easy and uniaxial refractive indices were also easily taken into account, the equations were conveniently used to analyze infrared spectra for the evaluation of molecular orientation in a thin film deposited on a transparent substrate.[5] The approximation theory, however, is not applicable to a film deposited on a metallic surface because both the first and third layers must be transparent, which means that this technique is not employable for the analysis of reflection−absorption (RA) spectra.[6]

To take uniaxial anisotropic structure into account without using approximation, other useful analytical approaches were proposed by various groups,[7−10] and representative ones having versatility are the 4 × 4 matrix methods individually proposed by Berreman[11] and Yeh.[12] Both methods have widely been used in both physics and chemistry fields for understanding the optical properties and chemical structure in thin films. For example, Parikh and Allara employed Yeh's method for simulation of infrared absorption spectra of LB films, and the empirical results were in an excellent agreement with the simulated ones involving uniaxial optical anisotropy.[13]

In this fashion, many different techniques have been proposed thus far, but all conventional techniques are analytical results of Maxwell's equations, which means that each technique is a different presentation of a dissolving process of Maxwell's equations, and there is no difference in principle between the techniques. For example, these techniques commonly take multiple reflections in each layer into account, which implies that each layer should be sandwiched by optically parallel and flat interfaces. This requirement is filled by LB films and self-assembled monolayers (SAMs),[14] but cast and dip-coated[15,16] films having an optically coarse surface are not suitable for the analytical techniques in principle.

To make a new way of understanding optical anisotropy by measuring spectra, a novel analytical concept was introduced: two spectra that correspond to the conventional transmission (IP) and RA (OP) spectra are measured simultaneously by using normal and virtual light, respectively.[17−20] This new technique was named multiple-angle incidence resolution spectrometry (MAIRS). The virtual light means that the electric-field oscillation is parallel to the traveling direction of the light. If we had the virtual light, then an RA-like spectrum that retrieves molecular vibrations in the OP direction can be measured by the normal-incidence transmission geometry. The normal-

---

* To whom correspondence should be addressed. E-mail: hasegawa@chem.titech.ac.jp.

10.1021/jp903769g CCC: $40.75

incidence transmission geometry is an exceptional geometry that the OP spectrum can directly be compared with the IP spectrum because both spectra have a common absorbance scale.[17−20] This is a characteristic of the development of MAIRS.

For the development of the virtual-light measurements, a totally different theoretical framework of "regression equation"[21,22] was employed instead of using the conventional rigorous equations. As described later, the core part of the MAIRS theory depends on the **R** matrix that contains weighting factors of the linear combination of the IP and OP single-beam spectra. When a regression equation is employed as the framework, the linear combination elucidates only a portion of the measured spectra, and the deduction of the **R** matrix directly from Maxwell's equations is close to impossible. In this sense, the **R** matrix is a magic matrix.

Through our application studies,[15,16,19−25] MAIRS has proved to work reliably to generate both IP and OP spectra from an identical sample on an FT-IR bench. Nevertheless, no theoretical analysis has been performed for understanding of MAIRS, which is definitely necessary to use the MAIRS spectra for reliable physicochemical discussion.

For this purpose, in the present study, the spectroscopic measurements have been replaced by physical expressions, where all the physical parameters are analytically derived from Maxwell's equations. As is often the case with spectroscopic analysis of stratified layers, the analysis has started from Yeh's transfer-matrix with a dielectric tensor,[2] which can be omitted from the present discussion because it has already been established. In our article, however, several original parameters were newly introduced to make the calculations simpler, which require descriptions of parameter determinations about the transfer-matrix. Therefore, the analytical discussion part will begin with the very basic electromagnetic theory.

Multiple-Angle Incidence Resolution Spectrometry Theory. Before beginning the theoretical analysis of MAIRS, the outline of the MAIRS theory should first be briefly introduced. The MAIRS technique is theorized on a regression equation, as presented in eq 1: a collection of single-beam spectra measured at different angles of incidence, $\mathbf{S}_{\text{obs}}$, is partially related to the linear combination of normal-incidence single-beam spectra, $\mathbf{s}_{\text{IP}}$ and $\mathbf{s}_{\text{OP}}$, by using the MAIRS matrix, **R**, whereas the residual part in $\mathbf{S}_{\text{obs}}$, which is not correlated to the linear combination, is discarded in **U**.[17−20]

$$\mathbf{S}_{\text{obs}} = \begin{pmatrix} r_{\text{IP},1} & r_{\text{OP},1} \\ r_{\text{IP},2} & r_{\text{OP},2} \\ \vdots & \vdots \end{pmatrix} \begin{pmatrix} \mathbf{s}_{\text{IP}} \\ \mathbf{s}_{\text{OP}} \end{pmatrix} + \mathbf{U} \equiv \mathbf{R} \begin{pmatrix} \mathbf{s}_{\text{IP}} \\ \mathbf{s}_{\text{OP}} \end{pmatrix} + \mathbf{U} \qquad (1)$$

Here **R**, which consisted of $r_{\text{IP},j}$ and $r_{\text{OP},j}$, is defined[17−20] as

$$\mathbf{R} = \left(\frac{4}{\pi}\right)^2 \begin{pmatrix} 1 + \cos^2\theta_j + \sin^2\theta_j \tan^2\theta_j & \tan^2\theta_j \\ \vdots & \vdots \end{pmatrix} \qquad (2)$$

In short, the collection of single-beam spectra is partially described by transmission "intensities" of transverse- and longitudinal-wave light rays ($\mathbf{s}_{\text{IP}}$ and $\mathbf{s}_{\text{OP}}$), which are both schematically irradiated onto the sample film perpendicularly.

The two single-beam spectra of $\mathbf{s}_{\text{IP}}$ and $\mathbf{s}_{\text{OP}}$ are calculated as a solution of the regression equation by the next equation[17]

$$\begin{pmatrix} \mathbf{s}_{\text{IP}} \\ \mathbf{s}_{\text{OP}} \end{pmatrix} = (\mathbf{R}^{\text{T}}\mathbf{R})^{-1}\mathbf{R}^{\text{T}}\mathbf{S}_{\text{obs}} \qquad (3)$$

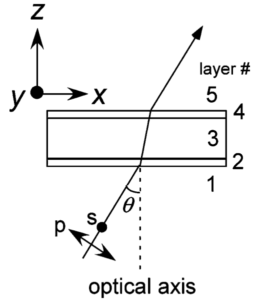

Figure 1. Schematic image of a five-layer medium and light transmitted through the medium.

This procedure is repeated for both sample and background measurements to yield two sets of $\mathbf{s}_{\text{IP}}$ and $\mathbf{s}_{\text{OP}}$, which finally yield IP and OP absorbance spectra.

In the present study, the validity of this technique will be proved theoretically. Therefore, we have to express the **S** matrix theoretically instead of using empirical values, and the algebraic calculation will be performed with eq 3 in the next Theoretical Analysis section.

Theoretical Analysis

1. Theoretical Fundamentals of Absorbance Spectra. The MAIRS analysis requires a collection of single-beam spectra that represent light-intensity variation against wavenumber at several angles of incidence. In the present analysis, therefore, the light intensity passed through the substrate covered with thin films must be theoretically formulated first. For this purpose, a stratified five-layer (air/film/substrate/film/air) medium is considered, as schematically drawn in Figure 1, in which the second and fourth layers correspond to the film layers and the third layer corresponds to the transparent substrate. The five-layer model represents a general symmetric double-sided LB film deposited on an infrared transparent substrate. In the present study, the optical axis is set aligned parallel to the z axis, and the traveling direction of light for the oblique-angle incidence transmission measurements is in the $x-z$ plane. For a wide variety of LB films, it is not a serious problem that the optical axis is parallel to the z axis. With this model, the electric field of the p polarization is within the $x-z$ plane, whereas that of the s polarization is parallel to the y axis.

The simplest model for analytical calculation should be a uniaxial model with the optical axis aligned to the z direction. Because MAIRS reveals only IP (x and y) and OP (z) spectra, the uniaxial model with the z-directed optical axis model would be good enough. Under this condition, the dielectric tensors of the thin films, $\boldsymbol{\varepsilon}_2$ and $\boldsymbol{\varepsilon}_4$, can be simply expressed as

$$\boldsymbol{\varepsilon}_2 = \begin{pmatrix} \varepsilon_{x,2} & 0 & 0 \\ 0 & \varepsilon_{y,2} & 0 \\ 0 & 0 & \varepsilon_{z,2} \end{pmatrix} = \boldsymbol{\varepsilon}_4 \qquad (4)$$

Here the uniaxial model requires $\varepsilon_{x,2} = \varepsilon_{y,2} \neq \varepsilon_{z,2}$, and the film thickness should be thin enough in comparison with the wavelength of the light, $d_2 = d_4 \ll \lambda_0$.

At an interface of two adjacent layers, a part of the incidental ray is reflected, and the rest transmits the interface as schematically represented in Figure 2. These phenomena are often expressed by using Fresnel's reflection law and the Snell's law, respectively.[26,27] The essentials of the phenomena should be expressed by the continuities of electric and magnetic fields at the interface. Here the p polarization is

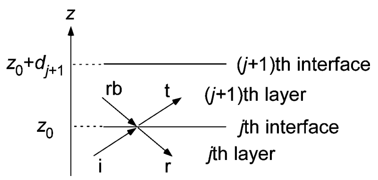

Figure 2. Schematic drawing of the layers and interfaces in the stratified layers.

modeled first, in which the magnetic-field oscillation is perfectly aligned in the y axis.

$$\begin{bmatrix} E^{\mathrm{i}}_{j,x} + E^{\mathrm{r}}_{j,x} \\ H^{\mathrm{i}}_{j,y} + H^{\mathrm{r}}_{j,y} \end{bmatrix} = \begin{bmatrix} E^{\mathrm{t}}_{j,x} + E^{\mathrm{rb}}_{j,x} \\ H^{\mathrm{t}}_{j,y} + H^{\mathrm{rb}}_{j,y} \end{bmatrix} \tag{5}$$

$E^{\mathrm{i}}_{j,x}$ is an amplitude of electric field aligned in the x direction at the jth interface, and the superscript, i, indicates that the ray is "incident" on the interface. In a similar manner, the reflected and transmitted rays are denoted by the superscripts r and t, respectively. The rest superscript, rb, represents a ray from multiple reflections in the layer (Figure 2). In this manner, the physical model takes multiple reflections into account for each layer except the first and the last layers.

Here the wavevector is decomposed into the amplitude, k, and the unit vector, **a**.

$$\mathbf{k} = k\mathbf{a} = k\begin{pmatrix} \sin\theta \\ 0 \\ \cos\theta \end{pmatrix} \equiv k\begin{pmatrix} a_x \\ a_y \\ a_z \end{pmatrix} \tag{6}$$

In the present study, a monochromatic plane wave is considered. Therefore, the derivative operators, ∇ and $\partial/\partial t$, can be replaced by $i k\mathbf{a}$ and $-i\omega$, respectively, which makes Maxwell's equations largely simplified, as follows by the use of $\mathbf{k} = k\mathbf{a}$.

$$\mathbf{D}\cdot\mathbf{a} = 0 \tag{7-1}$$

$$\mathbf{H}\cdot\mathbf{a} = 0 \tag{7-2}$$

$$\mathbf{a}\times\mathbf{H} = -\frac{\omega}{k}\mathbf{D} \tag{7-3}$$

$$\mathbf{a}\times\mathbf{E} = \frac{\omega}{k}\mathbf{B} \tag{7-4}$$

Under the uniaxial anisotropy with the optical axis perpendicular to the surface, p and s polarizations are coincident with the extraordinary and ordinary rays, respectively, in the uniaxial media.[2] When the incidental plane is set in the $x-z$ plane, $a_y = 0$ holds, and the extraordinary ray has a characteristic that the y component of electric field is zero ($E_y = 0$). Therefore, after eq 7-4, **B** is revealed to have only y component. Therefore, **H** can be written as $\mathbf{H} = H_y\mathbf{y}$, where **y** is the unit vector along the y axis, which means that p polarization in the present optical system is the same as TM polarization.

After eq 7-3, $\mathbf{H} \times \mathbf{a} = \omega/k\mathbf{D}$, **D** is deduced as

$$\mathbf{D} = \frac{\bar{n}}{c}H_y\begin{pmatrix} a_z \\ 0 \\ -a_x \end{pmatrix} \tag{8}$$

Here $\bar{n}$ is a reduced refractive index, which can be determined by Fresnel's equation (ellipsoid of anisotropic dielectric constants) to be[2,26]

$$\frac{1}{\bar{\boldsymbol{\varepsilon}}} = \frac{a_x^2}{\boldsymbol{\varepsilon}_z} + \frac{a_z^2}{\boldsymbol{\varepsilon}_x} \tag{9}$$

where $\varepsilon_0\boldsymbol{\varepsilon} = \varepsilon$ and $\bar{\boldsymbol{\varepsilon}} = \bar{n}^2$ holds.

By putting eq 8 into the next relationship

$$\mathbf{D} = \begin{pmatrix} \varepsilon_x & 0 & 0 \\ 0 & \varepsilon_x & 0 \\ 0 & 0 & \varepsilon_z \end{pmatrix}\mathbf{E} \Leftrightarrow \mathbf{E} = \begin{pmatrix} \varepsilon_x^{-1} & 0 & 0 \\ 0 & \varepsilon_x^{-1} & 0 \\ 0 & 0 & \varepsilon_z^{-1} \end{pmatrix}\mathbf{D} \tag{10}$$

the electric field is now expressed by using the magnetic field.

$$\mathbf{E} = \frac{\bar{n}}{c}H_y\begin{pmatrix} a_z\varepsilon_x^{-1} \\ 0 \\ -a_x\varepsilon_z^{-1} \end{pmatrix} \Rightarrow E_x = \frac{\bar{n}H_y}{c\varepsilon_x}a_z \tag{11}$$

As a result, eq 5 is largely simplified, which has no electric field term explicitly.

$$\begin{bmatrix} m_j & -m_j \\ 1 & 1 \end{bmatrix}\begin{bmatrix} H^{\mathrm{i}}_{j,y} \\ H^{\mathrm{r}}_{j,y} \end{bmatrix} = \begin{bmatrix} m_{j+1} & -m_{j+1} \\ 1 & 1 \end{bmatrix}\begin{bmatrix} H^{\mathrm{t}}_{j,y} \\ H^{\mathrm{rb}}_{j,y} \end{bmatrix} \tag{12}$$

where

$$m_j \equiv \frac{a^{\mathrm{i}}_{z,j}\sqrt{\bar{\boldsymbol{\varepsilon}}_j}}{c\varepsilon_{x,j}} \tag{13}$$

These formulas are a representation of the transfer-matrix method by Yeh for our case. With the matrix, transmission and reflection coefficients on any stratified layers can be calculated as long as the uniaxial anisotropy and the optical axis along the z axis are assumed.

The equations above hold at any interface, but no retardation is taken into account when the light travels across the layers. When the light having a wavelength of λ_0 in vacuum goes across a layer with a thickness of d_j, the phase retardation, δ_j, can simply be expressed as (Figure 2)

$$\begin{bmatrix} H^{\mathrm{i}}_{j+1,y} \\ H^{\mathrm{r}}_{j+1,y} \end{bmatrix} = \begin{bmatrix} \exp(i\delta_{j+1}) & 0 \\ 0 & \exp(-i\delta_{j+1}) \end{bmatrix}\begin{bmatrix} H^{\mathrm{t}}_{j,y} \\ H^{\mathrm{rb}}_{j,y} \end{bmatrix}$$
$$\text{where} \quad \delta_j \equiv 2\pi\frac{d_j}{\lambda_0} \tag{14}$$

When the matrices in the equations above are denoted as

$$\mathbf{N}_j \equiv \begin{bmatrix} H^{\mathrm{i}}_j \\ H^{\mathrm{r}}_j \end{bmatrix}, \quad \mathbf{F}_j \equiv \begin{bmatrix} H^{\mathrm{t}}_j \\ H^{\mathrm{rb}}_j \end{bmatrix}, \quad \mathbf{Q}_j \equiv \begin{bmatrix} m_j & -m_j \\ 1 & 1 \end{bmatrix}, \quad \text{and}$$
$$\mathbf{P}_j \equiv \begin{bmatrix} \exp(i\delta_{j+1}) & 0 \\ 0 & \exp(-i\delta_{j+1}) \end{bmatrix} \tag{15}$$

eqs 12−14 are simplified as

$$\mathbf{Q}_j\mathbf{N}_j = \mathbf{Q}_{j+1}\mathbf{F}_j \tag{16}$$

$$\mathbf{N}_{j+1} = \mathbf{P}_{j+1}\mathbf{F}_j \tag{17}$$

Therefore, the magnetic field intensities in the fifth layer are interrelated by the fourth interface to those in the first layer

$$\mathbf{N}_1 = \varphi_A\mathbf{P}_3^{-1}\varphi_B\mathbf{F}_4 \tag{18}$$

where

$$\varphi_A = \mathbf{Q}_1^{-1}\mathbf{Q}_2\mathbf{P}_2^{-1}\mathbf{Q}_2^{-1}\mathbf{Q}_3 \tag{19-1}$$

$$\varphi_B = \mathbf{Q}_3^{-1}\mathbf{Q}_2\mathbf{P}_2^{-1}\mathbf{Q}_2^{-1}\mathbf{Q}_1 \tag{19-2}$$

With these determinations, for example, $\mathbf{Q}_1^{-1}\mathbf{Q}_2$ is calculated to be the following

$$\mathbf{Q}_1^{-1}\mathbf{Q}_2 = \frac{1}{2m_1}\begin{pmatrix} 1 & m_1 \\ -1 & m_1 \end{pmatrix}\begin{pmatrix} m_2 & -m_2 \\ 1 & 1 \end{pmatrix} = t_{12p}^{-1}\begin{pmatrix} 1 & r_{12} \\ r_{12p} & 1 \end{pmatrix} \tag{20}$$

where

$$t_{ij\text{p}} \equiv \frac{2m_i}{m_i + m_j} \quad \text{and} \quad r_{ij\text{p}} \equiv \frac{m_i - m_j}{m_i + m_j} \quad (|i-j| = 1; \text{ otherwise see eq 23}) \tag{21}$$

The subscript "p" indicates that the parameters are for p polarization. Also note that there is no ray traveling in the $-z$ direction in the fifth layer, which means that $H_4^{\text{rb}} = 0$. As a result, $\mathbf{N}_1$ for the five-layer medium has been calculated to be

$$\frac{H^{\text{t}}_{4,y}}{H^{\text{i}}_{1,y}} = \frac{t_{13\text{p}}t_{31\text{p}}\exp(i\delta_3)}{1 - r^2_{31\text{p}}\exp(2i\delta_3)} \tag{22}$$

where

$$t_{13\text{p}} \equiv \frac{t_{12\text{p}}t_{23\text{p}}\exp(i\delta_2)}{1 + r_{12\text{p}}r_{23\text{p}}\exp(2i\delta_2)}, \quad t_{31\text{p}} \equiv \frac{t_{32\text{p}}t_{21\text{p}}\exp(i\delta_2)}{1 + r_{32\text{p}}r_{21\text{p}}\exp(2i\delta_2)}, \quad \text{and} \quad r_{31\text{p}} \equiv \frac{r_{32\text{p}} + r_{21\text{p}}\exp(2i\delta_2)}{1 + r_{32\text{p}}r_{21\text{p}}\exp(2i\delta_2)} \tag{23}$$

In our case, it is no problem to assume that the substrate thickness is much thicker than the wavelength of the light: $d_3 \gg \lambda_0$. With this approximation, the normalized light intensity can be averaged as

$$\frac{I^{\text{p}}_{\text{sam}}}{I^{\text{p}}_0} = \left|\frac{H^{\text{t}}_{4,y}}{H^{\text{i}}_{1,y}}\right|^2 = \frac{|t_{13\text{p}}t_{31\text{p}}|^2}{|1 - r^2_{31\text{p}}\exp(2i\delta_3)|^2} \xrightarrow{\text{averaged}} \frac{|t_{13\text{p}}t_{31\text{p}}|^2}{1 - |r_{31\text{p}}|^4} \quad (d_3 \gg \lambda_0) \tag{24}$$

To simplify eq 24 further, t_{13} and t_{31} are Taylor-expanded in terms of $\eta_2 \equiv d_2/\lambda_0$. Most analyte films are thin enough to the wavelength, and $\eta_2 \ll 1$ holds. When we consider the retardation term to be

$$\delta_j = k_{zj}d_j = k_j a_{zj} d_j = \frac{\omega}{c}\bar{n}_j a_{zj} d_j = 2\pi\eta_2\bar{n}_j\cos\theta_j \tag{25}$$

In the thin-film approximation, $\eta \ll 1$ holds well. If $\bar{n}_j\cos\theta_j$ is not so large (weak absorption), then $|\delta_j| \ll 1$ should also hold. Under the thin-film and weak absorption approximations, as a result, Taylor-expansion was performed.

$$t_{13\text{p}} = t_{130\text{p}}\left(1 + i\frac{1 - r_{12\text{p}}r_{23\text{p}}}{1 + r_{12\text{p}}r_{23\text{p}}}\delta\right) + o(\delta^2) \quad \text{where} \quad t_{130\text{p}} = \frac{t_{12\text{p}}t_{23\text{p}}}{1 + r_{12\text{p}}r_{23\text{p}}} \quad \text{and} \quad \delta \equiv \delta_3 \tag{26}$$

Another parameter, α_{13}, is introduced to make the calculation simpler.

$$\alpha_{13} = \frac{1 - r_{12\text{p}}r_{23\text{p}}}{1 + r_{12\text{p}}r_{23\text{p}}} = \frac{m_2^2 + m_1m_3}{(m_1 + m_3)m_2} = \alpha_{31} \equiv \alpha \tag{27}$$

Then

$$t_{13\text{p}} = t_{130\text{p}}(1 + i\alpha\delta + o(\delta^2)) \quad \text{and} \quad t_{31\text{p}} = t_{310\text{p}}(1 + i\alpha\delta + o(\delta^2)) \tag{28}$$

Therefore

$$|t_{13\text{p}}t_{31\text{p}}|^2 = t^2_{130\text{p}}t^2_{310\text{p}}\{1 + 4\,\text{Re}(i\alpha\delta) + o(\delta^2)\} \tag{29}$$

Here let us consider the continuity of wavevectors at an interface

$$k_{x1} = k_{xj} \leftrightarrow k_1a_{x1} = k_ja_{xj} \tag{30}$$

When $k_j = n_j\omega/c$ is considered, an expanded form of Snell's law for anisotropic media is obtained.

$$\bar{n}_j\sin\theta_j = n_1\sin\theta_1 \equiv X \tag{31}$$

This equation can be solved by employing Fresnel's equation (eq 9) to yield

$$\bar{\boldsymbol{\varepsilon}}_2 = \boldsymbol{\varepsilon}_{x2} + \left(1 - \frac{\boldsymbol{\varepsilon}_{x2}}{\boldsymbol{\varepsilon}_{z2}}\right)X^2 \tag{32}$$

With these parameters, the term of $\alpha\delta$ in eq 29 is calculated as follows

$$\alpha\delta = \frac{m_2^2 + m_1 m_3}{(m_1 + m_3)m_2}\delta = \frac{2\pi\eta\boldsymbol{\varepsilon}_{x2}(m_2^2 + m_1 m_3)}{m_1 + m_3} \tag{33}$$

By considering that m_1, m_3, and η are all real numbers, eq 33 is a little organized.

$$\mathrm{Re}(i\alpha\delta) = \frac{2\pi\eta}{m_1 + m_3}\mathrm{Re}[i\boldsymbol{\varepsilon}_x(m_2^2 + m_1 m_3)] = \frac{2\pi\eta}{m_1 + m_3}\{\mathrm{Re}(i\boldsymbol{\varepsilon}_x m_2^2) + m_1 m_3\,\mathrm{Re}(i\boldsymbol{\varepsilon}_x)\} \tag{34}$$

where $\boldsymbol{\varepsilon}_x \equiv \boldsymbol{\varepsilon}_{x2} = \boldsymbol{\varepsilon}_{x4}$ is newly introduced. Because $\boldsymbol{\varepsilon}_x m_2^2$ can be calculated to be

$$\boldsymbol{\varepsilon}_x m_2^2 = \boldsymbol{\varepsilon}_x \frac{\bar{n}_2^2 \cos^2\theta_2}{\boldsymbol{\varepsilon}_x^2} = \frac{\bar{\boldsymbol{\varepsilon}}_2}{\boldsymbol{\varepsilon}_x}(1 - \sin^2\theta_2) = \frac{\bar{\boldsymbol{\varepsilon}}_2 - X^2}{\boldsymbol{\varepsilon}_x} = 1 - \frac{X^2}{\boldsymbol{\varepsilon}_z} \tag{35}$$

then

$$\mathrm{Re}(i\boldsymbol{\varepsilon}_x m_2^2) = -X^2\,\mathrm{Re}\left(\frac{i}{\boldsymbol{\varepsilon}_z}\right) = -X^2\frac{\boldsymbol{\varepsilon}_z''}{|\boldsymbol{\varepsilon}_z|^2} = -X^2\,\mathrm{Im}\left(-\frac{1}{\boldsymbol{\varepsilon}_z}\right) \tag{36}$$

holds. Re $(i\boldsymbol{\varepsilon}_x)$ in eq 34 can be rewritten as

$$\mathrm{Re}(i\boldsymbol{\varepsilon}_x) = -\boldsymbol{\varepsilon}_x'' = -\mathrm{Im}(\boldsymbol{\varepsilon}_x) \tag{37}$$

As a result, $|t_{13\mathrm{p}}t_{31\mathrm{p}}|^2$ has been analytically deduced as

$$|t_{13\mathrm{p}}t_{31\mathrm{p}}|^2 = t_{130\mathrm{p}}^2 t_{310\mathrm{p}}^2(1 - \Phi) \tag{38}$$

where

$$\Phi \equiv \frac{8\pi\eta}{m_1 + m_3}\left(m_1 m_3\,\mathrm{Im}(\boldsymbol{\varepsilon}_x) + X^2\,\mathrm{Im}\left(-\frac{1}{\boldsymbol{\varepsilon}_z}\right)\right) \tag{39}$$

In a similar manner, $|r_{31\mathrm{p}}|^4$ was also Taylor-expanded by the use of the thin-film and weak-absorption approximations, and the following formula has analytically been obtained

$$|r_{31\mathrm{p}}|^4 = r_{310\mathrm{p}}^4(1 + C) \quad \text{where} \quad r_{310\mathrm{p}} = \frac{r_{32\mathrm{p}} + r_{21\mathrm{p}}}{r_{32\mathrm{p}}r_{21\mathrm{p}} + 1} = \frac{m_3 - m_1}{m_1 + m_3} \tag{40}$$

and

$$C \equiv \frac{8\eta m_3}{m_3^2 - m_1^2}\left(m_1^2\,\mathrm{Im}(\boldsymbol{\varepsilon}_x) - X^2\,\mathrm{Im}\left(-\frac{1}{\boldsymbol{\varepsilon}_z}\right)\right) \tag{41}$$

Now, we are at last ready for the calculation of transmission of p polarization for the sample, $T^{\mathrm{p}} \equiv T^{\mathrm{p}}_{\mathrm{sam}}/T^{\mathrm{p}}_{\mathrm{BG}}$, with which an absorbance spectrum would readily be calculated later. Here related parameters are also introduced for the convenience of calculation.

$$T^{\mathrm{p}}_{\mathrm{sam}} \equiv \frac{I^{\mathrm{p}}_{\mathrm{sam}}}{I^{\mathrm{p}}_0}, \quad T^{\mathrm{p}}_{\mathrm{BG}} \equiv \frac{I^{\mathrm{p}}_{\mathrm{BG}}}{I^{\mathrm{p}}_0}, \quad \varphi \equiv \frac{T^{\mathrm{s}}_{\mathrm{BG}}}{T^{\mathrm{p}}_{\mathrm{BG}}}, \quad \gamma \equiv \frac{I^{\mathrm{s}}_0}{I^{\mathrm{p}}_0} \tag{42}$$

T is a transmission spectra normalized by the work function that depends on the spectrometer and γ corresponds to the polarization dependence of the spectrometer. With these parameters, the p-polarized transmission spectrum is analytically calculated, followed by the Taylor expansion

$$T^{\mathrm{p}} = \frac{|t_{13\mathrm{p}}t_{31\mathrm{p}}|^2}{t_{130\mathrm{p}}^2 t_{310\mathrm{p}}^2}\frac{1 - r_{310\mathrm{p}}^4}{1 - |r_{31\mathrm{p}}|^4} = (1 - \Phi)\frac{1 - r_{310\mathrm{p}}^4}{1 - (1 + C)r_{310\mathrm{p}}^4} \cong (1 - \Phi)\{1 + \Gamma_{\mathrm{p}}C\} \tag{43}$$

where

$$\Gamma_{\mathrm{p}} \equiv \frac{r_{310\mathrm{p}}^4}{1 - r_{310\mathrm{p}}^4} \tag{44}$$

Because C and Φ are both first-order functions of η, T^{p}can be simplified in terms of η as

$$T^{\mathrm{p}} = (1 - \Phi)\{1 + \Gamma_{\mathrm{p}}C\} + o(\eta^2) = 1 - \Phi + \Gamma_{\mathrm{p}}C + o(\eta^2) \equiv 1 - \Pi_{\mathrm{p}} + o(\eta^2) \tag{45-1}$$

here

$$\Pi_{\mathrm{p}} = \Phi - \Gamma_{\mathrm{p}}C = 8\pi\eta\,\mathrm{Im}(\boldsymbol{\varepsilon}_x)\cdot a^{\mathrm{p}} + 8\pi\eta\,\mathrm{Im}\left(-\frac{1}{\boldsymbol{\varepsilon}_z}\right)\cdot b^{\mathrm{p}} \tag{45-2}$$

and the newly appeared coefficients are defined as

$$a^{\mathrm{p}} = \frac{m_1 m_3}{m_1 + m_3} - \Gamma_{\mathrm{p}}\frac{2m_3 m_1^2}{m_3^2 - m_1^2}, \quad b^{\mathrm{p}} = \frac{X^2}{m_1 + m_3} - \Gamma_{\mathrm{p}}\frac{2m_3 X^2}{m_3^2 - m_1^2} \tag{46}$$

In a very similar manner, s-polarization-related parameters can also be deduced. Important results are selectively presented below.

$$T^{\mathrm{s}} = 1 - G - F\Gamma_{\mathrm{s}} + o(\eta^2) \equiv 1 - \Pi_{\mathrm{s}} + o(\eta^2) \quad \text{where} \quad \Gamma_{\mathrm{s}} \equiv \frac{r_{310\mathrm{s}}^4}{1 - r_{310\mathrm{s}}^4} \tag{47}$$

$$G = \frac{8\pi\eta}{\xi_1 + \xi_3}\,\mathrm{Im}(\boldsymbol{\varepsilon}_x),\ F = \frac{16\pi\eta\xi_3}{\xi_3^1 - \xi_1^1}\,\mathrm{Im}(\boldsymbol{\varepsilon}_x) = \frac{16\pi\eta\xi_3}{\boldsymbol{\varepsilon}_3 - \boldsymbol{\varepsilon}_1}\,\mathrm{Im}(\boldsymbol{\varepsilon}_x) \tag{48}$$

$$\Pi_{\mathrm{s}} = 8\pi\eta\,\mathrm{Im}(\boldsymbol{\varepsilon}_x)a^{\mathrm{s}} \quad \text{where} \quad a^{\mathrm{s}} = \frac{1}{\xi_1 + \xi_3} + \Gamma_{\mathrm{s}}\frac{2\xi_3}{\boldsymbol{\varepsilon}_3 - \boldsymbol{\varepsilon}_1} \quad \text{and} \quad \xi_j = n_j \cos\theta_j \tag{49}$$

Then, the light intensity of unpolarized transmitted ray through the sample, $I_{\mathrm{sam}}^{\mathrm{u}}$, is formulated as follows

$$\begin{aligned} I_{\mathrm{sam}}^{\mathrm{u}} &= I_{\mathrm{sam}}^{\mathrm{p}} + I_{\mathrm{sam}}^{\mathrm{s}} = T_{\mathrm{sam}}^{\mathrm{p}}I_0^{\mathrm{p}} + T_{\mathrm{sam}}^{\mathrm{s}}I_0^{\mathrm{s}} = \\ &T^{\mathrm{p}}T_{\mathrm{BG}}^{\mathrm{p}}I_0^{\mathrm{p}} + T^{\mathrm{s}}T_{\mathrm{BG}}^{\mathrm{s}}I_0^{\mathrm{s}} = (T^{\mathrm{p}} + T^{\mathrm{s}}\varphi\gamma)I_0^{\mathrm{p}}T_{\mathrm{BG}}^{\mathrm{p}} = \\ &\{(1 + \varphi\gamma) - (\varphi\gamma\Pi_s + \Pi_{\mathrm{p}})\}I_0^{\mathrm{p}}T_{\mathrm{BG}}^{\mathrm{p}} \end{aligned} \tag{50}$$

In the same manner, the light intensity of unpolarized transmitted ray through the background, $I_{\mathrm{BG}}^{\mathrm{u}}$, is formulated by taking the three-layer model (no film layer) into account.

$$I_{\mathrm{BG}}^{\mathrm{u}} = (1 + \varphi\gamma)I_0^{\mathrm{p}}T_{\mathrm{BG}}^{\mathrm{p}} \tag{51}$$

Therefore, an absorbance spectrum for the normal-incidence transmission measurements, A^{u}, is calculated from the sample and background spectra by using $\ln(1 - x) \cong -x$.

$$\begin{aligned} A^{\mathrm{u}} &= -\log\left(\frac{I_{\mathrm{sam}}^{\mathrm{u}}}{I_{\mathrm{BG}}^{\mathrm{u}}}\right) = -\frac{1}{\ln 10}\ln\left(\frac{I_{\mathrm{sam}}^{\mathrm{u}}}{I_{\mathrm{BG}}^{\mathrm{u}}}\right) \\ &= -\frac{1}{\ln 10}\ln\left(1 - \frac{\Pi_{\mathrm{p}} + \varphi\gamma\Pi_{\mathrm{s}}}{1 + \varphi\gamma}\right) \\ &\cong \frac{1}{\ln 10}\left(\frac{1}{1 + \varphi\gamma}\Pi_{\mathrm{p}} + \frac{\varphi\gamma}{1 + \varphi\gamma}\Pi_{\mathrm{s}}\right) \end{aligned} \tag{52}$$

For the normal-incidence transmission measurements, $\theta_1 = 0$ holds, which means that b^{p} in eq 46 is zero because X in eq 31 becomes zero. Therefore, the component of $\mathrm{Im}(-1/\boldsymbol{\varepsilon}_z)$ that appeared in A^{u} is removed, and only the rest of the component of $\mathrm{Im}(\boldsymbol{\varepsilon}_x)$ remains, which is a characteristic of normal-incidence transmission spectrometry.[28]

Let us consider a case in which the analyte film is deposited on a high refractive index substrate, which is a normal condition of the original infrared MAIRS.[29] In the case of germanium substrate, for example, the refractive index (n_3) in the mid-infrared region is roughly 4.0. With these parameters, the numerically calculated result has been obtained, as presented below

$$A^{\mathrm{u}} \cong \frac{1}{\ln 10}\left(\frac{1}{1 + \varphi\gamma}\Pi_{\mathrm{p}} + \frac{\varphi\gamma}{1 + \varphi\gamma}\Pi_{\mathrm{s}}\right) = 0.2794 \cdot 8\pi\eta\,\mathrm{Im}(\boldsymbol{\varepsilon}_x) \tag{53}$$

The coefficient of 0.2794 will be useful for examining the MAIRS-IP spectrum, as shown in the next section.

In a similar manner, an RA spectrum can also be analytically deduced. As is well known, RA spectrometry retrieves spectra of the $\eta\,\mathrm{Im}(-1/\boldsymbol{\varepsilon}_z)$ component selectively,[28] which is complementary to the transmission spectrometry. In this article, the deduction process is omitted.

2. Analysis of Multiple-Angle Incidence Resolution Spectrometry. Now, fundamental parts are all ready, and we are moving to analysis of MAIRS. To do that, the theoretically deduced light intensity is put in the $\mathbf{S}_{\mathrm{obs}}$ matrix of MAIRS theory, and the optimal solution is calculated by eq 3.

To make the calculation simpler, the $\mathbf{R}$ matrix is rewritten as follows

$$\mathbf{R} = \left(\frac{4}{\pi}\right)^2\begin{pmatrix} 1 + \cos^2\theta_j + \sin^2\theta_j\tan^2\theta_j & \tan^2\theta_j \\ \vdots & \vdots \end{pmatrix} \equiv \left(\frac{4}{\pi}\right)^2\begin{pmatrix} x_j & y_j \\ \vdots & \vdots \end{pmatrix} \equiv c(\mathbf{X} \quad \mathbf{Y}) \tag{54}$$

With this formulation, the calculation steps are as follows

$$(\mathbf{R}^{\mathrm{T}}\mathbf{R})^{-1} = \frac{1}{c^2\zeta}\begin{bmatrix} \mathbf{Y}^{\mathrm{T}}\mathbf{Y} & -\mathbf{X}^{\mathrm{T}}\mathbf{Y} \\ -\mathbf{Y}^{\mathrm{T}}\mathbf{X} & \mathbf{X}^{\mathrm{T}}\mathbf{X} \end{bmatrix} \quad \text{where} \quad \zeta \equiv (\mathbf{X}^{\mathrm{T}}\mathbf{X})(\mathbf{Y}^{\mathrm{T}}\mathbf{Y}) - (\mathbf{X}^{\mathrm{T}}\mathbf{Y})(\mathbf{Y}^{\mathrm{T}}\mathbf{X}) \tag{55-1}$$

$$(\mathbf{R}^{\mathrm{T}}\mathbf{R})^{-1}\mathbf{R}^{\mathrm{T}} = \frac{1}{c\zeta}\begin{bmatrix} \mathbf{Z}_{\mathrm{IP}}^{\mathrm{T}} \\ \mathbf{Z}_{\mathrm{OP}}^{\mathrm{T}} \end{bmatrix} \tag{55-2}$$

$$\mathbf{Z}_{\mathrm{IP}}^{\mathrm{T}} \equiv \mathbf{Y}^{\mathrm{T}}\mathbf{Y}\mathbf{X}^{\mathrm{T}} - \mathbf{X}^{\mathrm{T}}\mathbf{Y}\mathbf{Y}^{\mathrm{T}}, \quad \mathbf{Z}_{\mathrm{OP}}^{\mathrm{T}} \equiv -\mathbf{Y}^{\mathrm{T}}\mathbf{X}\mathbf{X}^{\mathrm{T}} + \mathbf{X}^{\mathrm{T}}\mathbf{X}\mathbf{Y}^{\mathrm{T}} \tag{55-3}$$

$$\therefore \begin{bmatrix} \mathbf{s}_{\mathrm{IP}} \\ \mathbf{s}_{\mathrm{OP}} \end{bmatrix} = \frac{1}{c\zeta}\begin{bmatrix} \mathbf{Z}_{\mathrm{IP}}^{\mathrm{T}}\mathbf{S}_{\mathrm{obs}} \\ \mathbf{Z}_{\mathrm{OP}}^{\mathrm{T}}\mathbf{S}_{\mathrm{obs}} \end{bmatrix} \tag{55-4}$$

$$T_{\mathrm{IP}} = \frac{s_{\mathrm{sam}}^{\mathrm{IP}}}{s_{\mathrm{BG}}^{\mathrm{IP}}} = \frac{\mathbf{Z}_{\mathrm{IP}}^{\mathrm{T}}\mathbf{S}_{\mathrm{sam}}^{\mathrm{obs}}}{\mathbf{Z}_{\mathrm{IP}}^{\mathrm{T}}\mathbf{S}_{\mathrm{BG}}^{\mathrm{obs}}} \quad \text{and} \quad T_{\mathrm{OP}} = \frac{s_{\mathrm{sam}}^{\mathrm{OP}}}{s_{\mathrm{BG}}^{\mathrm{OP}}} = \frac{\mathbf{Z}_{\mathrm{OP}}^{\mathrm{T}}\mathbf{S}_{\mathrm{sam}}^{\mathrm{obs}}}{\mathbf{Z}_{\mathrm{OP}}^{\mathrm{T}}\mathbf{S}_{\mathrm{BG}}^{\mathrm{obs}}} \tag{56}$$

For the ratio calculation, either $I_{\mathrm{sam}}^{\mathrm{u}}$ or $T_{\mathrm{sam}}^{\mathrm{p}}$ can be put in $\mathbf{S}_{\mathrm{sam}}^{\mathrm{obs}}$, and the simpler form, $T_{\mathrm{sam}}^{\mathrm{p}}$, is chosen in the present study.

$$\begin{aligned} T_{\mathrm{IP}} &= \frac{\sum_{\theta} Z_{\mathrm{IP}}\{(1 + \varphi\gamma) - (\varphi\gamma\Pi_{\mathrm{s}} + \Pi_{\mathrm{p}})\}I_0^{\mathrm{p}}T_{\mathrm{BG}}^{\mathrm{p}}}{\sum_{\theta} Z_{\mathrm{IP}}I_0^{\mathrm{p}}T_{\mathrm{BG}}^{\mathrm{p}}(1 + \varphi\gamma)} \\ &= 1 - \frac{\sum_{\theta} Z_{\mathrm{IP}}(\varphi\gamma\Pi_{\mathrm{s}} + \Pi_{\mathrm{p}})T_{\mathrm{BG}}^{\mathrm{p}}}{\sum_{\theta} Z_{\mathrm{IP}}(1 + \varphi\gamma)T_{\mathrm{BG}}^{\mathrm{p}}} \end{aligned} \tag{57}$$

The sigma with θ represents summation for all angles of incidence. Under the thin-film approximation, the absorbance can easily be deduced in a way similar to the calculation of eq 45-2 as

$$A_{\mathrm{IP}} = -\ln T_{\mathrm{IP}} \cong \frac{\sum_{\theta} Z_{\mathrm{IP}}(\varphi\gamma\Pi_{\mathrm{s}} + \Pi_{\mathrm{p}})T^{\mathrm{p}}_{\mathrm{BG}}}{\sum_{\theta} Z_{\mathrm{IP}}(1 + \varphi\gamma)T^{\mathrm{p}}_{\mathrm{BG}}} = 8\pi\eta\,\mathrm{Im}(\boldsymbol{\varepsilon}_x)h_x^{\mathrm{IP}} + 8\pi\eta\,\mathrm{Im}\left(-\frac{1}{\boldsymbol{\varepsilon}_z}\right)h_z^{\mathrm{IP}} \quad (58\text{-}1)$$

where

$$h_x^{\mathrm{IP}} = \frac{\sum Z_{\mathrm{IP}}(a^{\mathrm{p}} + \varphi\gamma a^{\mathrm{s}})T^{\mathrm{p}}_{\mathrm{BG}}}{\sum Z_{\mathrm{IP}}(1 + \varphi\gamma)T^{\mathrm{p}}_{\mathrm{BG}}}, \quad h_z^{\mathrm{IP}} = \frac{\sum Z_{\mathrm{IP}}b^{\mathrm{p}}T^{\mathrm{p}}_{\mathrm{BG}}}{\sum Z_{\mathrm{IP}}(1 + \varphi\gamma)T^{\mathrm{p}}_{\mathrm{BG}}} \quad (58\text{-}2)$$

The calculation of A_{OP} is easily performed by the replacement of the subscripts of IP by OP.

$$A_{\mathrm{OP}} = 8\pi\eta\,\mathrm{Im}(\boldsymbol{\varepsilon}_x)h_x^{\mathrm{OP}} + 8\pi\eta\,\mathrm{Im}\left(-\frac{1}{\boldsymbol{\varepsilon}_z}\right)h_z^{\mathrm{OP}} \quad (59\text{-}1)$$

where

$$h_x^{\mathrm{OP}} = \frac{\sum Z_{\mathrm{OP}}(a^{\mathrm{p}} + \varphi\gamma a^{\mathrm{s}})T^{\mathrm{p}}_{\mathrm{BG}}}{\sum Z_{\mathrm{OP}}(1 + \varphi\gamma)T^{\mathrm{p}}_{\mathrm{BG}}}, \quad h_z^{\mathrm{OP}} = \frac{\sum Z_{\mathrm{OP}}b^{\mathrm{p}}T^{\mathrm{p}}_{\mathrm{BG}}}{\sum Z_{\mathrm{OP}}(1 + \varphi\gamma)T^{\mathrm{p}}_{\mathrm{BG}}} \quad (59\text{-}2)$$

Of note is that the parameters of h_x^{IP}, h_z^{IP}, h_x^{OP}, and h_z^{OP} depend on n_1, n_3, θ_j, and γ only, which are all free from optical parameters of the analyte thin film. In this fashion, the MAIRS-IP and -OP spectra for a five-layer medium have both readily been deduced by using the in-plane ($\mathrm{Im}(\boldsymbol{\varepsilon}_x)$) and out-of-plane ($\mathrm{Im}(-1/\boldsymbol{\varepsilon}_z)$) spectra. These explicit expressions of MAIRS spectra are the first report.

As mentioned in the previous section, the normal-incidence transmission spectrum is a function of $\mathrm{Im}(\boldsymbol{\varepsilon}_x)$ only because b^{p} in eq 45-2 is zero. If this transmission spectrum quantitatively agrees with the MAIRS-IP spectrum, then h_x^{IP} should be close to the factor of 0.2794, as found in eq 53. We employed $n_1 = 1$ and $n_3 = 4$ for the calculation of h_x^{IP} with the use of a wide variety of the angles of incidence. As a result, we have found that h_x^{IP} always stays at about 0.2790 irrespective of the choice of angles. This strongly proves that a MAIRS-IP spectrum should be measured very stably, and it quantitatively agrees with the conventional normal-incidence transmission spectrum.

On the other hand, the MAIRS-OP spectrum is expected to correspond to the RA spectrum.[17−20] As stated in the previous section, the RA spectrum selectively observes the $\eta\,\mathrm{Im}(-1/\boldsymbol{\varepsilon}_z)$ component, whereas the rest of the $\mathrm{Im}(\boldsymbol{\varepsilon}_x)$ component is largely diminished.[28] Because the RA spectrometry has a surface enhancement factor in comparison with the transmission spectrometry, the absolute value of absorbance of an RA spectrum cannot directly be compared with the corresponding MAIRS-OP spectrum. The surface selection rule of the MAIRS-OP spectrum, however, should be the same as that of RA spectrometry, which implies that the MAIRS-OP spectrum should also largely depend on the $\eta\,\mathrm{Im}(-1/\boldsymbol{\varepsilon}_z)$ component, whereas h_x^{OP} should be small enough. In short, $h_x^{\mathrm{OP}} \ll h_z^{\mathrm{OP}}$ should hold.

With the same optical parameters used for the MAIRS-IP examination, the two coefficients of h_x^{OP} and h_z^{OP} were calculated. It has been revealed, as a result, that these two coefficients largely depend on the range of the angle of incidence. In our former studies, we employed the range from 45 through 10° by 7° (or sometime 5°) steps for obtaining satisfying results for analyses on a germanium or silicon substrate.[17−20] Our present numerical calculation of the coefficients has revealed that $h_x^{\mathrm{OP}} \ll h_z^{\mathrm{OP}}$ holds enough with the experimental condition. In this manner, a MAIRS-OP spectrum has been proven to correspond to the RA spectrum.

When a low refractive index substrate such as $n_3 = 1.5$ was used, the MAIRS-IP spectrum was still calculated to be stable, whereas the OP spectrum was found to be largely degraded, and $h_x^{\mathrm{OP}} \ll h_z^{\mathrm{OP}}$ did not hold at all. These calculation results are perfectly consistent with a theoretical analysis discussed on a regression equation when the p-MAIRS technique was proposed.[30,31] In the case of p-MAIRS, a similar theoretical analysis based on the classical electromagnetic theory can be performed, which will be reported later.

Summary

The unique spectroscopic measurement theory of MAIRS using a high refractive index substrate has inductively been analyzed on the basis of Maxwell's equations. The rigorous analytical calculations of MAIRS-IP and -OP spectra have revealed that both spectra can be expressed as a linear combination of $\mathrm{Im}(\boldsymbol{\varepsilon}_x)$ and $\mathrm{Im}(-1/\boldsymbol{\varepsilon}_z)$ functions. The weighting factors of the two functions were numerically calculated by the use of optical parameters that are practically used in our daily experiments. As a result, the MAIRS-IP spectrum is very robust against the choice of the angle range of incidence, whereas the OP spectrum is largely influenced by the experimental condition. Fortunately, however, our experimental parameters were found to be very good, which makes the MAIRS measurements reliable, as expected through our previous experiments.

In addition, the MAIRS proves to be degraded when a low refractive index substrate is used for the measurements, which has long been pointed out by our previous p-MAIRS theory.[30,31] In this manner, the original MAIRS technique[17] has first been understood from the viewpoint of the classical electromagnetic theory.

Acknowledgment. This work was financially supported by Grant-in-Aid for Scientific Research (B) (no. 20350035) and Priority Areas (no. 21020012) from the Ministry of Education, Science, Sports, Culture, and Technology, Japan and also by Iketani Science and Technology Foundation, Japan, to whom our great thanks are due.

References and Notes

(1) Abeles, F. *Ann. Phys.* **1950**, *50*, 596–640.

(2) Yeh, P. *Optical Waves in Layered Media*; Wiley: Hoboken, NJ, 1998.

(3) Hansen, W. N. *J. Opt. Soc. Am.* **1968**, *58*, 380–390.

(4) Hansen, W. N. Reflection Spectroscopy of Adsorbed Layers. In *Symposium on Optical Studies of Adsorbed Layers at Interfaces (1970: London, England)*; Symposia of the Faraday Society no. 4; Faraday Society: London, 1971; pp 27−35.

(5) Mielczarski, J. A.; Yoon, R. H. *Langmuir* **1991**, *7*, 101–108.

(6) Umemura, J. Reflection-Absorption Spectroscopy of Thin Films on Metallic Substrates. In *Handbook of Vibrational Spectroscopy*, Chalmers, J. M., Griffiths, P. R., Eds.; John Wiley: Chichester, U.K., 2002; Vol. 2, pp 982−998.

(7) Mansuripur, M. *J. Appl. Phys.* **1990**, *67*, 6466–6475.

(8) Nicolau, G. *Cerc. Energ. Electr.* **1973**, *23*, 47–58.

(9) Lewandowski, S. J. *J. Phys. A: Gen. Phys.* **1971**, *4*, 197–205.

(10) Mosteller, Jr, L. P; Wooten, F. *J. Opt. Soc. Am.* **1968**, *58*, 511–518.

(11) Berreman, D. W. *J. Opt. Soc. Am.* **1972**, *62*, 502–510.

(12) Yeh, P. *Surf. Sci.* **1980**, *96*, 41–53.

(13) Parikh, A. N.; Allara, D. L. *J. Chem. Phys.* **1992**, *96*, 927–945.

(14) Ulman, A. *Chem. Rev.* **1996**, *96*, 1533–1554.

(15) Matsunaga, M.; Suzuki, T.; Yamamoto, K.; Hasegawa, T. *Macromolecules* **2008**, *41*, 5780–5784.

(16) Kakuda, H.; Okada, T.; Hasegawa, T. *J. Phys. Chem. B* **2008**, *112*, 12940–12945.

(17) Hasegawa, T. *J. Phys. Chem. B* **2002**, *106*, 4112–4115.

(18) Hasegawa, T. *Anal. Bioanal. Chem.* **2003**, *375*, 18–19.

(19) Hasegawa, T. *Anal. Bioanal. Chem.* **2007**, *388*, 7–15.

(20) Hasegawa, T. *Appl. Spectrosc. Rev.* **2008**, *43*, 181–201.

(21) Hasegawa, T.; Kakuda, H.; Yamada, N. *J. Phys. Chem. B* **2005**, *109*, 4783–4787.

(22) Hasegawa, T.; Nakano, Y.; Ishii, Y. *Anal. Chem.* **2006**, *87*, 1739–1742.

(23) Hasegawa, T.; Iiduka, Y.; Kakuda, H.; Okada, T. *Anal. Chem.* **2006**, *78*, 6121–6125.

(24) Kakuda, H.; Hasegawa, T.; Tanaka, T.; Tanaka, K.; Shionoya, M. *Chem. Phys. Lett.* **2005**, *415*, 172–175.

(25) Hasegawa, T.; Sato, Y.; Kakuda, H.; Li, C.; Orbulescu, J.; Leblanc, R. M. *J. Phys. Chem. B* **2008**, *109*, 1391–1396.

(26) Born, M.; Wolf, E. *Principles of Optics*, 5th ed.; Elsevier: Amsterdam, 1975; p 709.

(27) Hecht, E. *Optics*, 2nd ed.; Addison-Wesley: Reading, MA, 1990; p 84.

(28) Tolstoy, V. P.; Chernyshova, I. V.; Skryshevsky, V. A. *Handbook of Infrared Spectroscopy of Ultrathin Films*; John Wiley: Chichester, U.K., 2003.

(29) Hasegawa, T.; Matsumoto, L.; Kitamura, S.; Amino, S.; Katada, S.; Nishijo, J. *Anal. Chem.* **2002**, *74*, 6049–6054.

(30) Hasegawa, T. *Anal. Chem.* **2007**, *79*, 4385–4389.

(31) Hasegawa, T.; Itoh, Y.; Kasuya, A. *Anal. Chem.* **2008**, *80*, 5630–5634.

JP903769G